iJRASET
International Journal For Research in Applied Science and Engineering Technology



INTERNATIONAL JOURNAL FOR RESEARCH

IN APPLIED SCIENCE & ENGINEERING TECHNOLOGY

Volume: 9 **Issue:** VII **Month of publication:** July 2021

DOI: https://doi.org/10.22214/ijraset.2021.36367

www.ijraset.com

Call: 08813907089 | E-mail ID: ijraset@gmail.com

International Journal for Research in Applied Science & Engineering Technology (IJRASET)
ISSN: 2321-9653; IC Value: 45.98; SJ Impact Factor: 7.429
Volume 9 Issue VII July 2021- Available at www.ijraset.com

Sliding Mode Control for Chaotic Oscillations in SMIB Power System

Tandel Zankhana[1], Rathod Ajit[2]
[1, 2]*Deperament of Electrical Engieenering, S.S.E.C Engineering collage, Bhavnagar*

Abstract: ***Power systems may revelation the harmful and undesirable chaotic phenomenon in certain conditions. This project describes the control of a chaotic oscillation in power system. Chaos may lead the power system to voltage instability and voltage collapse when voltage stability conditions are broken. Chaotic oscillations are very sensitive to parameter and initial conditions of power system. Many controllers are projected in practical to suppress the chaos and avoid voltage collapse. In this thesis, a Conventional Sliding Mode Control is applied for removal of chaotic oscillations. The aim of the controller is to remove the chaotic oscillations and bring the order to the nonlinear system. It is also shown that the proposed controller assurances the system state convergence to their desired ethics. To demonstrate the effectiveness of the projected controller, MATLAB Programming is done.***

Keywords: Chaotic oscillations, SMIB, Conventional Sliding Mode Control

I. INTRODUCTION

Generally, the electric power systems are embraced of three-phase AC systems which is operating basically at constant voltages. Voltage stability refers as the ability of the system to maintain steady acceptable voltages at all buses of the power system under normal operating conditions and after being subjected to some disturbances too. Due to increase in the loads demand, faults on the system or any other changes which is affecting the system conditions, the disturbances produced.

When a disturbance acting on the system causes an overpowering and progressive change in the bus voltages, the power system comes into voltage instability state. A low unacceptable voltage profile in a significant part of the power system may be led by The sequence of events associated voltage instability which led the system to the voltage avalanche[1].

In past decades, significant research and development work has been undertaken to gain a better insight and develop analytical tools for system stability studies. Though interconnected transmission networks result in economical operation and increased reliability through mutual support, they also contribute to an increased complexity of stability problems. The complex transmission network may worsen the consequences of instability in such cases[2].

In the past twenty years, power system instability is one of the main reasons for large-scale blackouts all over the world. Modern power system is forced to operate close to its stability limit due to the growth of power demand and other constraints for structuring new power plants and transmission lines. Recently, electric power systems have become huger and more complicated as stability problems have become more complex as interconnections become more extensive.

Power system is a very complex nonlinear system. So, there may be the chance of exhibiting unstable behaviour. This complex nonlinear system frequently leads to problem that are related to its safety and shows unstable operations. Power system comes into transient stage when the disturbance happens. If the disturbance is small then continuous oscillation follows and if the disturbance is large then the system may come into chaotic behaviour[3].

Many researchers studies the chaotic marvel in power system which were mainly focused on the effect of chaotic oscillations in power system. The main cause of these oscillations and its relationship with power system instability were also studied in [9-13].

During the analysis of stability of nonlinear system, it is very crucial to study the nature and dynamics of its response. It is obvious that a complex nonlinear system shows chaotic oscillations under certain initial conditions. It makes the system dynamically unstable, causes severe problems and ultimately leads to operational instability.

To supress these chaotic oscillations and voltage instability, different kind of the sliding mode controllers are used [6]. Chattering-free time scale separation SMC was applied in [8] to power system chaos suppression. CSMC and Super Twisting SMC are implemented in [11] for the chaos suppression.

In the early 1960s, Russian scientists invented Sliding Mode Control and it is known from Variable Structure Control (VSC) and also stated in the article of Utkin in 1970s [4]. SMC has a simplicity and robustness in contrast to system uncertainties and instabilities. That's why it studied widely and effectually for the implementation in control problems[5].

©IJRASET: All Rights are Reserved

ISSN: 2321-9653; IC Value: 45.98; SJ Impact Factor: 7.429
Volume 9 Issue VII July 2021- Available at www.ijraset.com

II. SINGLE MACHINE INFINITE BUS POWER SYSTEM MODELLING

A. Dynamic Model Of The Power System

Under some consideration, a three-bus system is consisted by the power system as shown in Fig. 1. The infinite busbar is represented by E_0, V_0 and θ_0. The Generator model is represented by E_m, V_m and θ_m, the load bus voltage and phase angle are represented by V_L and δ. This considered system also involves an induction motor with a PQ load in parallel. [10]

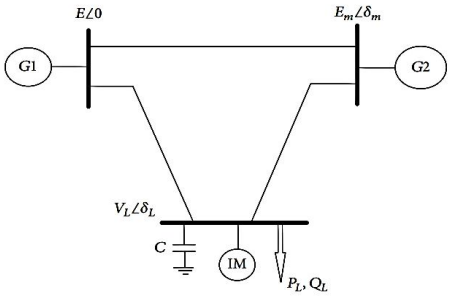


Fig. 1. Considered three-bus power system

The rotor motion of the generator is specified via the swing equation, [13][14]

$M.\ddot{\delta}_m + d_m.\dot{\delta}_m = P_m - P_e$ (1)

$\dot{\delta}_m = \omega_m$ (2)

The generated electrical power,

$P_e = - E_m^2 Y_m \sin(\theta_m) - E_m V_L Y_m \sin(\delta - \delta_m + \theta_m)$ (3)

Using (1), (3) and (2), we get

$M.\dot{\omega}_m = - d_m \omega_m + P_m + E_m V_L Y_m \sin(\delta - \delta_m - \theta_m) + E_m^2 Y_m \sin(\theta_m)$ (4)

B. Model Of The Power System Load

The load model comprises of a dynamic induction motor representation for industrial load which is in parallel with a constant P-Q load and a constant impedance load representing residential plus commercial load. Here, load demands are voltage and frequency dependent.

P (scheduled) = $P_0 + P_1 + k_{p\omega}\dot{\delta} + k_{pv}(V_L + TV_L)$

Q(scheduled) = $Q_0 + Q_1 + k_{q\omega}\dot{\delta} + k_{qv}.V_L + k_{qv2}.V_L^2$

(5)

where,

P_0, Q_0 = The constant real and reactive powers of the motor respectively

P_1, Q_1 = P-Q loads that can be varied for getting load flow result

T = Time constant of the motor

$k_{p\omega}$, $k_{q\omega}$, k_{pv}, k_{qv} and k_{qv2} = Empirical constants that characterize the load

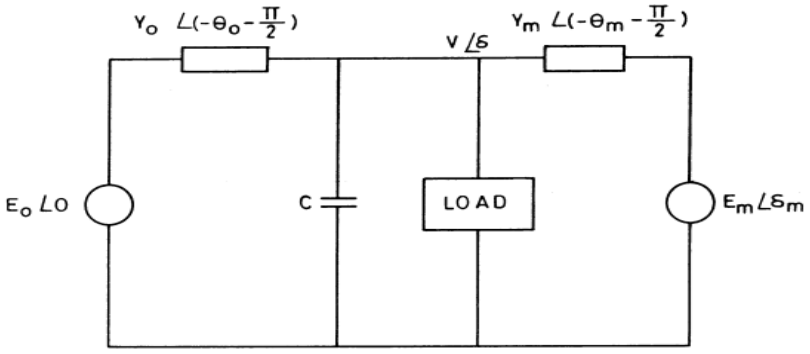


Fig. 2. A modest power system

©IJRASET: All Rights are Reserved

ISSN: 2321-9653; IC Value: 45.98; SJ Impact Factor: 7.429
Volume 9 Issue VII July 2021- Available at www.ijraset.com

Initially, the load flow has a flat start with $V_L = 1$ pu and $\delta = 0$. After that new $P_{(sch)}$ and $Q_{(sch)}$ are calculated with $V_L = 0$ and $\delta = 0$.

Figure is modelled as Thevenin equivalent circuit to make it convenient to account for the capacitor by adjusting E_0 and Y_0 instead of including the capacitor in the circuit. Therefore, the voltage, admittance and angle of Thevenin equivalent circuit can be expressed as,

$$E_0' = \frac{E_0}{\sqrt{c^2 Y_0^{-2} - 2cY_0^{-1}.\cos\theta_0 + 1}}$$

$$Y_0' = \sqrt{Y_0^2 - 2cY_0 \cos\theta_0 + c^2}$$

$$\theta_0' = \theta_0 + \tan^{-1}\frac{cY_0^{-1}\sin\theta_0}{1 - cY_0^{-1}\cos\theta_0}$$

The real power of the load bus is being supplied through the network is expressed by,

$$P = -E_0' Y_0' V_L \sin(\delta + \theta_0') - E_m V_L Y_m \sin(\delta - \delta_m + \theta_m) + (Y_0' \sin(\theta_0) + Y_m \sin(\theta_m)).V_L^2 \quad (6)$$

The reactive power of the load bus is being supplied through the network is expressed by,

$$Q = E_0' Y_0' V_L \cos(\delta + \theta_0') + E_m V_L Y_m \cos(\delta - \delta_m + \theta_m) - (Y_0' \cos(\theta_0) + Y_m \cos(\theta_m).V_L^2 \quad (7)$$

Using the above equations (5), (6) and (7), we get

$$k_{gw}.\dot{\delta} = E_0' Y_0' V_L \cos(\delta + \theta_0') + E_m V_L Y_m \cos(\delta - \delta_m + \theta_m) - k_{gv}.V_L - Q_0 - Q_1 - (k_{gv2} + Y_0' \cos(\theta_0) + Y_m \cos(\theta_m)).V_L^2 \quad (8)$$

$$T.\dot{V}_L.k_{gw}.k_{gv} = k_{gw} k_{gv2} V_L^2 + (k_{gw} k_{gv} - k_{gw} k_{gv}) V_L - k_{gw}(E_0' Y_0' V_L \sin(\delta + \theta_0') + E_m V_L Y_m \cos(\delta - \delta_m + \theta_m)) + k_{gw}((Y_0' \sin(\theta_0')) + Y_m \sin(\theta_m)).V_L^2 - P_0 - P_1) - k_{gw}(E_0' Y_0' V_L \cos(\delta + \theta_0') + E_m V_L Y_m \cos(\delta - \delta_m + \theta_m)) + k_{gw}((Y_0' \cos(\theta_0') + Y_m \cos(\theta_m)) V_L^2 + Q_0 + Q_1) \quad (9)$$

By gathering the equation (2), (4), (8) and (9) represent the power system dynamic model.

C. Calculation of Equilibrium Points

By setting the left-hand side of equations (2), (4), (8) and (9) to zero and solving the non-linear algebraic equations by the Newton–Raphson method, the steady state equilibrium points δ_m^0, ω_m^0, δ^0, V_L^0 can be calculated.

By taking the first partial derivatives of the right-hand side of equation (2), (4), (8) and (9), the Jacobian matrix of the load flow equations can be calculated. The determinant of the Jacobian becomes zero when these equilibrium points become the saddle node bifurcation points.

$$\det(J) = 0 \quad (10)$$

©IJRASET: All Rights are Reserved

By equating the determinant of (J) to as well as by neglecting higher order terms and assuming that the cosine of a small angle is equal to one and the sine of a small angle to be equal to the angle itself in det(J) will take the following term:

$$- k_{qv} + E_0' Y_0' + E_m Y_m - 2(k_{qv2} + Y_0' + Y_m).V_L = 0$$

$$V_L = \frac{(- k_{qv} + E_0' Y_0' + E_m Y_m)}{2(k_{qv2} + Y_0' + Y_m)} \quad (11)$$

$$Q_1 = \frac{(- k_{qv} + E_0' Y_0' + E_m Y_m)^2}{4(k_{qv2} + Y_0' + Y_m)} - Q_0 \quad (12)$$

From equation (9), the load active power at bifurcation is obtained.

$$P_1 = \frac{1}{k_{qw}}(k_{pw}\, k_{qv2}\, V_L^2 + (k_{pw}\, k_{qv} - k_{qw}\, k_{pv})\, V_L - k_{qw}(P_0 - P) + k_{pw}(Q_0 + Q_1 - Q)) \quad (13)$$

The other equilibrium points δ, δ_m and ω_m can be obtained by solving the nonlinear equations (2), (4), (8) and (9) iteratively.

By substituting the parameters values given in [10] in (4.4), (4.8) and (4.9), the equilibrium points for V_L, Q and P can be obtained. The parameters of the generator are such that $Y_m = 5$, $\theta_m = -5$, $E_m = 1$, $P_m = 1$, $d_m = 0.05$, and $M = 0.3$. Te parameters of the network are such that $Y_0 = 20$, $\theta_0 = -5$, $E_0 = 1$, $c = 12$, $Y_0' = 8$, $\theta_0' = -12$, and $E_0' = 2.5$ Te parameters of the load are such that $k_{qv2} = 0.4$, $k_{pv} = 0.3$, $k_{qw} = -0.03$, $k_{qv} = -2.8$, $k_{qv2} = 2.1$, $T = 8.5$, $P_0 = 0.6$, $Q_0 = 1.3$. All the parameter values are in per unit except the angles which are in radians.

By applying these values of parameters, the power system model can be written as,

$$\dot{\delta}_m = \omega_m$$
$$\dot{\omega}_m = p_1 V_L \sin(\delta - \delta_m + p_2) + p_3 \omega_m + p_4$$
$$\dot{\delta} = p_5 V_L \cos(\delta - \delta_m - p_2) - p_6 V_L \cos(\delta - p_7) + p_8 V_L^2 + p_9 V_L + p_{10}\, Q_1 + p_{11} + u_1$$
$$\dot{V}_L = p_{12}\, V_L \cos(\delta - \delta_m - p_{13}) + p_{14} V_L \cos(\delta - p_{15}) + p_{16} V_L^2 + p_{17}\, V_L + p_{18} Q_1 + p_{19} + u_2 \quad (14)$$

Here the values of parameters p1-p19 are as following:

p1 = 16.66667, p2 = 0.087266, p3 = −0.16667,

p4 = 1.88074, p5 = −166.6667, p6 = −666.66667,

p7 = 0.20944, p8 = 496.87181, p9 = −93.3333,

p10 = 33.33333, p11 = 43.33333, p12 = 26.21722,

p13 = 0.01241, p14 = 104.868887, p15 = 0.13458,

p16 = −78.7638, p17 = 14.52288, p18 = −5.22876,

p19 = −7.03268.

The state variables x_1, x_2, x_3, x_4 is taken instead of δ_m, ω_m, δ, V_L respectively. So, the state variable x_1-x_4 is written in such that $[x_1\ x_2\ x_3\ x_4]^T = [\delta_m\ \omega_m\ \delta\ V_L]^T$.

©IJRASET: All Rights are Reserved

Hence, the power system dynamic model is determined by following expressions:

$$\dot{x}_1 = x_2$$
$$\dot{x}_2 = p_1 x_4 \sin(x_3 - x_1 + p_2) + p_3 x_2 + p_4$$
$$\dot{x}_3 = p_5 x_4 \cos(x_3 - x_1 - p_2) - p_6 x_4 \cos(x_3 - p_7) + p_8 x_4^2 + p_9 x_4 + p_{10} Q_1 + p_{11} + u_1$$
$$\dot{x}_4 = p_{12} x_4 \cos(x_3 - x_2 - p_{13}) + p_{14} x_4 \cos(x_3 - p_{15}) + p_{16} x_4^2 + p_{17} x_4 + p_{18} Q_1 + p_{19} + u_2 \quad (15)$$

The fourth-order model (15) of the power system is simulated when $u_1 = u_2 = 0$ and with Q_1=11.37 to obtain the results without using controller.

The thesis's main aim is to design controllers meant for the power system so that chaotic oscillation can be suppressed.
For that let x_{1d}, x_{2d}, x_{3d} and x_{4d} represent the desired values of x_1, x_2, x_3, x_4 respectively which satisfy the following two equations:

1) $x_{2d} = 0$

2) $p_1 x_{4d} \sin(x_{3d} - x_{1d} + p_2) + p_4 = 0 \quad (16)$

D. Transformation Model

To signify the errors between actual and desired states of the system, the transformation model is obtained. So, the following transformation is proposed to facilitate the design of the controller:

$$z_1 = x_1 - x_{1d}$$
$$z_2 = x_2$$
$$z_3 = p_1 x_4 \sin(x_3 - x_1 + p_2) + p_1 x_{4d} \sin(x_{3d} - x_{1d} + p_2) + p_3 x_2$$
$$z_4 = x_3 - x_{3d} \quad (17)$$

Here, $z_1(t)$, $z_2(t)$, $z_3(t)$ and $z_4(t)$ assurances that when they converge to zero at $t \to \infty$, then the system states $x_1(t)$, $x_2(t)$, $x_3(t)$ and $x_4(t)$ congregate to their desired ethics, respectively.

The system model is given by the expression (15) by applying the transformation (17) can be described as,

$$\dot{z}_1 = z_2$$
$$\dot{z}_2 = z_3$$
$$\dot{z}_3 = f_1 + \overline{u_1}$$
$$\dot{z}_4 = f_2 + \overline{u_2} \quad (18)$$

where,

$$f_1 = p_1 p_{12} x_4 \sin(x_3 - x_1 + p_2) \cos(x_3 - x_1 + p_{13}) + p_1 (p_{14} x_4 \cos(x_3 - p_{15}) + p_{16} x_4^2 + p_{17} x_4 + p_{18} Q_1 + p_{19}) \sin(x_3 - x_1 + p_2) + p_1 x_4 \cos(x_3 - x_1 + p_2) (p_5 x_4 \cos(x_3 - x_1 - p_2) - p_6 x_4 \cos(x_3 - p_7) + p_8 x_4^2 + p_9 x_4 + p_{10} Q_1 + p_{11}) + x_3 (p_1 x_4 \sin(x_3 - x_1 + p_2) + p_3 x_2 + p_4)$$

$$f_2 = p_5 x_4 \cos(x_3 - x_1 - p_2) - p_6 x_4 \cos(x_3 - p_7) + p_8 x_4^2 + p_9 x_4 + p_{10} Q_1 + p_{11}$$
$$\overline{u_1} = p_1 u_2 \sin(x_3 - x_1 + p_2) + p_1 u_1 x_4 \cos(x_3 - x_1 + p_2)$$

$$\overline{u_2} = u_1 \quad (19)$$

©IJRASET: All Rights are Reserved

The transformed model (17) is used to design the controller. The controllers will be designed to power the state variables $z_1(t)$, $z_2(t)$, $z_3(t)$ and $z_4(t)$ to congregate them to zero as $t\to\infty$, so that the system states $x_1(t)$, $x_2(t)$, $x(t)$ and $x_4(t)$ meet to their desired ethics.

E. Design of a Conventional SMC to suppress the chaotic Oscillations

The first step for the choice of the sliding surfaces, is the design of sliding mode controllers.

Here two sliding surfaces are design for the two inputs of the power system. For that let β_1, β_2, η_1, η_2, K_1 and K_2 be positive scalars. Hence, the sliding surface S_1 and S_2 are formed as,

$$S_1 = z_3 + \beta_1 z_1 + \beta_2 z_2 \quad (20)$$

$$S_2 = z_4 \quad (21)$$

Theorem: By applying the sliding mode controller $\overline{u_1}$ and $\overline{u_2}$ to the transformed model (17), the state variables $z_1(t)$, $z_2(t)$, $z_3(t)$ and $z_4(t)$ ensures its convergence to zero as $t\to\infty$.

$$\overline{u_1} = -f_1 - \beta_1 z_2 - \beta_2 z_3 - \eta_1(z_3 + \beta_1 z_1 + \beta_2 z_2) - K_1 \text{sign}(z_3 + \beta_1 z_1 + \beta_2 z_2) \quad (22)$$

$$\overline{u_2} = -f_2 - \eta_2 z_4 - K_2 \text{sign}(z_4) \quad (23)$$

Proof:

Differentiating (20) and (21) with respect to time (t) and using (18),

$$\dot{S_1} = \dot{z_3} + \beta_1 \dot{z_1} + \beta_2 \dot{z_2} = f_1 + \overline{u_1} + \beta_1 z_2 + \beta_2 z_3 \quad (24)$$

By substituting the value of $\overline{u_1}$ and $\overline{u_2}$ from (22) and (23) respectively,

$$\dot{S_1} = -\eta_1 S_1 - K_1 \text{sign}(S_1) \quad (25)$$

$$\dot{S_2} = \dot{z_4} = f_2 + \overline{u_2} = -\eta_2 S_2 - K_2 \text{sign}(S_2) \quad (26)$$

The expression descried below is satisfy by above dynamic equations (25) and (26):

$$S_i \dot{S_i} = -\eta_i S_i^2 - K_i S_i \text{sign}(S_i) = -\eta_i S_i^2 - K_i |S_i|; \quad \text{for } i = 1, 2. \quad (27)$$

When $S_i \neq 0$, the dynamic equations (25) and (26) assurance that $S_i \dot{S_i} < 0$ for (i= 1, 2). Whatever the trajectories associated with the discontinuous dynamics (25) and (26) show a finite time reachability to zero from any primary condition which providing the scalars β_1, β_2, η_1, η_2, K_1 and $K_2$are positive scalars where the gains K_1 and K_2 are strictly positive and large. Hence, to reach the surfaces $S_1 = 0$ and $S_2 = 0$ for finite time the dynamic equations (25) and (26) give the assurance.

Determined that $S_1 = 0$ for finite time, by the equation $z_3 + \beta_1 z_1 + \beta_2 z_2 = 0$, the variables $z_1(t)$, $z_2(t)$ and $z_3(t)$ are overseen after such finite time. Since $z_1(t)$ will asymptotically converge to zero, the decision is made here from the transformed system (17) that $z_2(t)$ and $z_3(t)$ will asymptotically converge to 0 as $t\to\infty$. As S_2 is driven to zero in finite time, $z_4(t)$ will congregate to zero in finite time.

So, the conclusion is made that the sliding mode controller inputs (25)-(26) gave the assurance of the state variables $z_1(t)$, $z_2(t)$, $z_3(t)$ and $z_4(t)$ to zero as $t\to\infty$. Thus, the controller (25)-(26) guarantee that the asymptotic convergence of the states of $x_1(t)$, $x_2(t)$, $x_3(t)$ and $x_4(t)$ to their desired ethics for $t\to\infty$.

To reduce the chattering associated with the proposed sliding mode controller, the switching function sign can be replaced by the saturation function, such that,

$$\text{Sat}(S_i) = \begin{cases} \text{sign}(S_i), & S_i > \epsilon \\ S_i/\epsilon, & S_i \leq \epsilon \end{cases} \quad (28)$$

with ϵ is a small positive number.

©IJRASET: All Rights are Reserved

International Journal for Research in Applied Science & Engineering Technology (IJRASET)
ISSN: 2321-9653; IC Value: 45.98; SJ Impact Factor: 7.429
Volume 9 Issue VII July 2021- Available at www.ijraset.com

III. RESULT ANALYSIS OF THE DYNAMIC POWER SYSTEM WITHOUT CONTROLLER

The results of the programming without controller are shown in figures 1 to 5. Figure 1 and 2 show the waveforms of the machine angle δ_m and the speed deviation ω_m v/s time without applying any controller respectively.

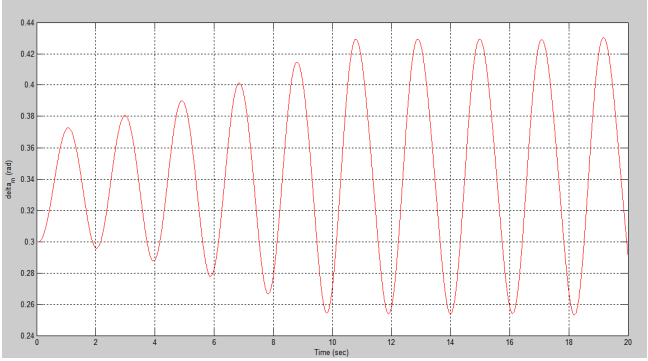


Fig. 1. The machine power angle δ_m v/s time without controller

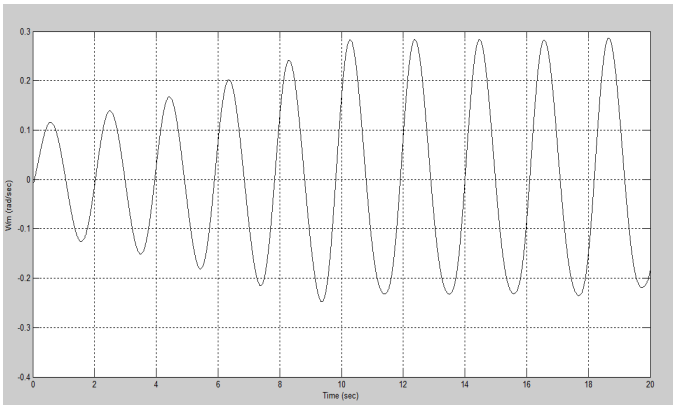


Fig. 2. The speed deviation ω_m v/s time without controller

The graphs of angle δ and load voltage V_L v/s time without applying any controller are shown in figure 3 and 4 respectively. These graphs clearly showed that the chaotic oscillations are present in them in the presence of the disturbance. So, to mitigate these chaotic oscillations from the system, the implementation of the appropriate controller should be necessary.

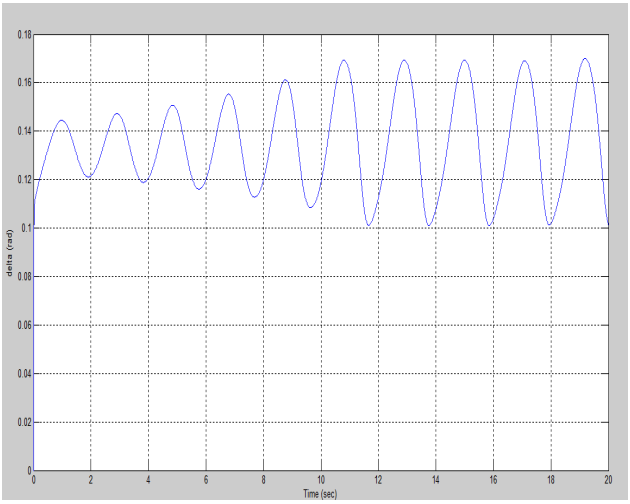


Fig. 3. The load power angle δ v/s time without controller

©IJRASET: All Rights are Reserved

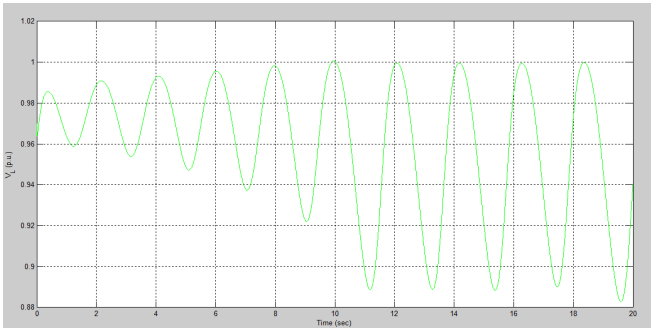


Fig. 4. The load voltage V_L v/s time without controller

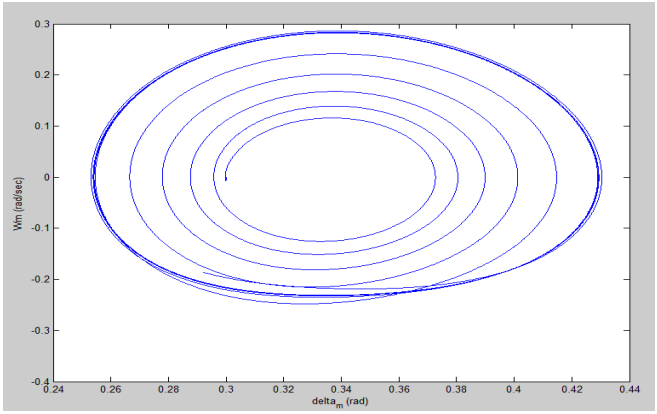


Fig. 5. The machine power angle δ_m v/s ω_m the speed deviation without controller

Here, the graph of angle δ_m versus ω_m without controller is shown in figure 5 which represent that in finite-time, the system states are not congregated near their desired ethics because of the chaotic oscillations. For the system congregate to their desired ethics by eliminate these oscillations, controller is applied in the system.

For the programming of the dynamic power system model (15) with controller, the control inputs u_1 and u_2 should be variable with the disturbing parameter Q_1. So, the programming results are obtained for system with control inputs $u_1$and u_2 as given in (22) and (23) and Q_1 = 11.37.

IV. RESULT ANALYSIS OF THE DYNAMIC POWER SYSTEM WITH CONTROLLER

The results of the programming with controller are shown in figures 6 to 12. Figure 6 and 7 show the waveforms of the machine power angle δ_m versus time and the speed deviation ω_m versus time with controller respectively.

It is cleared from these figures 6 and 7 that whatever the oscillation produced, is suppressed when SMC controller is used into the closed loop system. The machine power angle δ_m and the speed deviation ω_m of the system converges to their desired value within 2 to 5 sec which means the proposed controller works well.

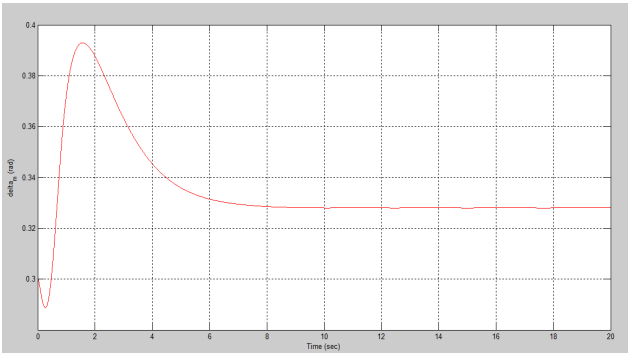


Fig. 6. The machine power angle δ_m v/s time with controller

©IJRASET: All Rights are Reserved

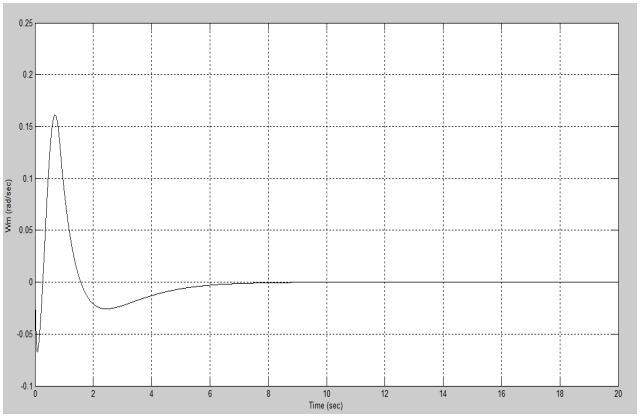


Fig. 7. The speed deviation ω_m v/s time with controller

The graphs of the load power angle δ and the load voltage V_L versus time with controller are shown in figure 8 and 9 respectively. These graphs clearly showed that the chaotic oscillations well suppressed as SMC is applied into the closed loop system but the responses suffer a little bit from chattering problem.

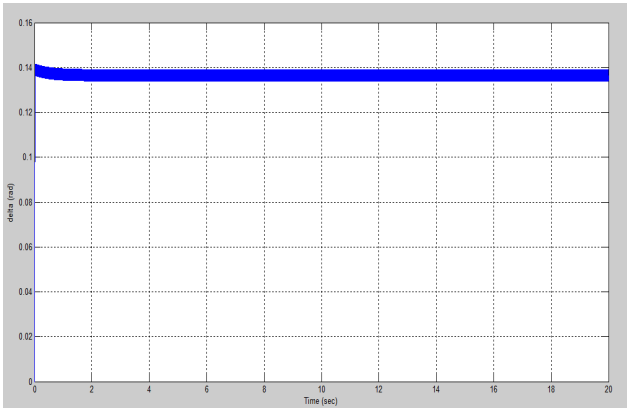


Fig. 8. The load power angle δ v/s time with controller

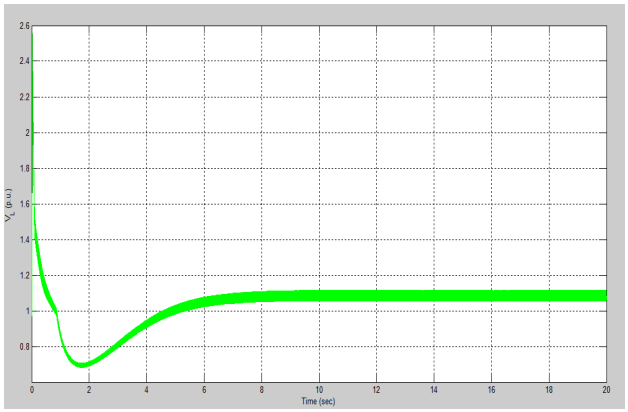


Fig. 5.9. The load voltage V_L v/s time with controller

Here, figure 10 and 11 show the graphs of inputs of CSMC u_1 and u_2 v/s time, in which the chattering problem is observed. Here, u_2 produces an aggressive chattering problem. To suppression this chattering problem, higher order SMC can be used by means of obtaining better results.

©IJRASET: All Rights are Reserved

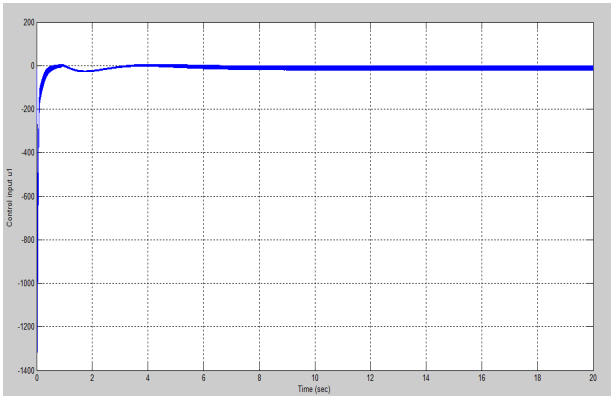


Fig. 10. The input of CSMC u_1 v/s time

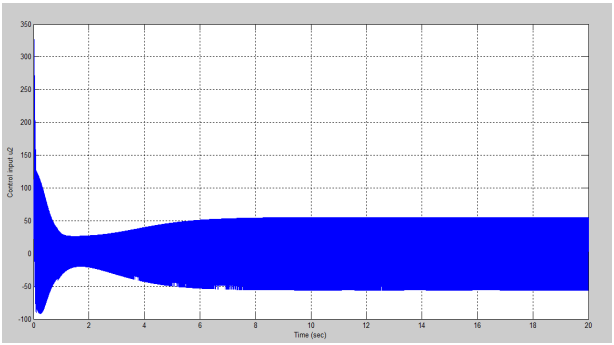


Fig. 11. The input of CSMC u_2 v/s time

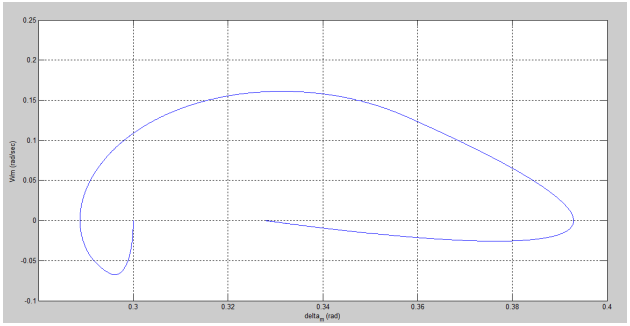


Fig. 12. The machine power angle δ_m v/s ω_m the speed deviation with controller

The graph of the machine angle δ_m v/s the speed deviation ω_m with CSMC is shown in figure 6 which shows that the system states are converged near their desired ethics in finite time as controller is applied. So, it can be concluded that the proposed CSMC works well but its transient responses suffer a little bit because of chattering problem. Nevertheless, this problem is overcome by using the higher order SMC.

V. CONCLUSION

In this paper, the problem of controlling chaos in a power system is studied in this thesis, for which the three- bus power system model is used. It is obvious that there might be present the chaotic oscillation under certain initial conditions which is very sensitive to the initial conditions and system parameter as power system is a complex nonlinear system. So, any small changes to them can break the stable oscillations. Here, Conventional SMC is used to suppress these chaotic oscillations. Because of this controller, the states of the dynamic power system converge to their desired values in finite time and concluded that the proposed controller works well.

©IJRASET: All Rights are Reserved

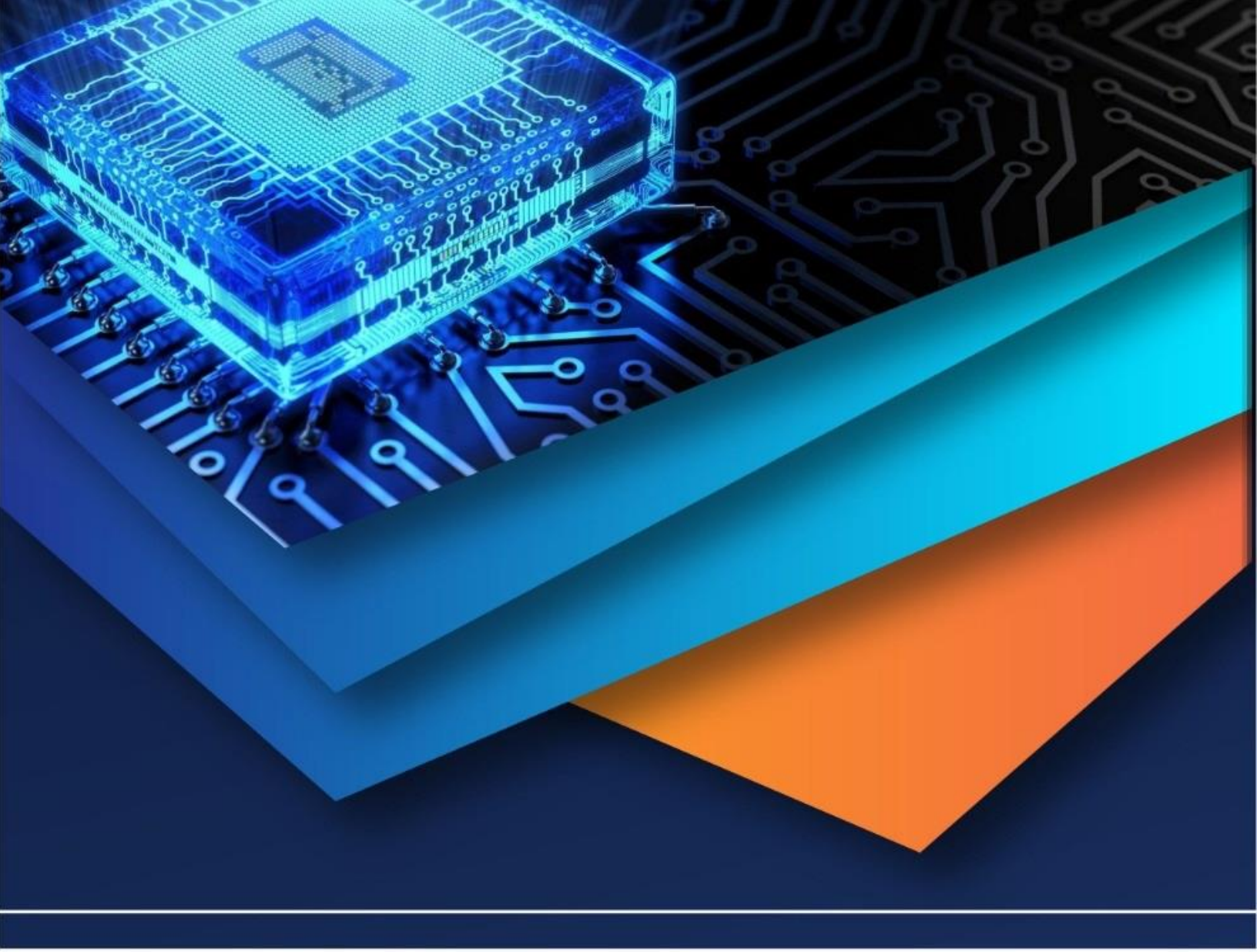
VI. FUTURE SCOPE

In future, the problem of suppressing chaotic oscillations, chattering phenomenon and peak overshoot will done by using other types of sliding mode control schemes like Higher Order SMC, Super Twisting Second Order SMC, Advanced SMC, Terminal SMC and Discrete-time SMC as well as observer-based controllers.

REFERENCES

[1] P.Kundur, Power System Stability and Control. Electric power research Institute, McGraw-Hill Inc., New York, USA, 1994.
[2] D. S. Kumar, A. Sharma, D. Srinivasan, and T. Reindl, "Definition and Classification of power system stability" IEEE Transactions On Power Systems, Vol. 19, No. 2, May 2004.
[3] R. H. Clark, "System Dynamics and Modeling," pp. 163., 1988.
[4] V. I. Utkin, "Variable Structure Systems with Sliding Modes," IEEE Trans. Automat. Contr., vol. 22, no. 2, pp. 212–222, 1977.
[5] L. Pasteur and R. Koch, "Advanced Sliding Mode Control for Mechanical Systems: Design, Analysis and MATLAB Simulation © Tsinghua University Press, Beijing and Springer-Verlag Berlin Heidelberg 2012
[6] Y. Shtessel, C. Edwards, L. Fridman, and A. Levant, Sliding mode control and observation. 2014.
[7] M. T. Do, "Sliding Mode Learning Control and its Applications," 2014.
[8] A. Swikir, "Chattering Analysis of Conventional and Super Twisting SMC Algorithm," no. 1, pp. 98–102, 2016.
[9] Y. Yu, H. Jia, P. Li, and J. Su, "Power System Instability And Chaos," no. June, pp. 24–28, 2002.
[10] I. Dobson, H.-D. Chiang, J. S. Torp, and L. Fekih-Ahmed, "Model of voltage collapse in electric power systems," in Proceedings of the 27th IEEE Conference on Decision and Control, pp. 2104–2109, Austin, Tex, USA, December 1988.
[11] J. Ni, L. Liu, C. Liu, and X. Hu, "Chattering-Free Time Scale Separation SMC Design with Application to Power System Chaos Suppression," vol. 2016, 2016.
[12] V. Utkin, A. Poznyak, Y. Orlov, and A. Polyakov, "Conventional and high order sliding mode control," J. Franklin Inst., vol. 357, no. 15, pp.
[13] A. Teshome and E. Esiyok, "Distance to voltage collapse through second-order eigenvalue sensitivity technique," Int. J. Electr. Power Energy Syst., vol. 17, no. 6, pp. 425–431, 1995.

©IJRASET: All Rights are Reserved



10.22214/IJRASET

45.98

IMPACT FACTOR: 7.129

IMPACT FACTOR: 7.429

INTERNATIONAL JOURNAL FOR RESEARCH

IN APPLIED SCIENCE & ENGINEERING TECHNOLOGY

Call : 08813907089 (24*7 Support on Whatsapp)